

# Using multifunctional nanorods to determine the influence of size, magnetism and transferrin in gene delivery to cultured cells.

A.K. Salem,<sup>1,2</sup> P.C. Searson,<sup>2</sup> and K.W. Leong<sup>1\*</sup>

<sup>1</sup>Department of Biomedical Engineering, <sup>2</sup>Department of Materials Science and Engineering, Johns Hopkins University, Baltimore, Maryland 21218

\*To whom correspondence should be addressed: kleong@bme.jhu.edu

Delivering DNA into cells is a fundamental aim in gene therapy. This can be achieved by viral or non-viral delivery systems. Viral systems, whilst highly efficient display high toxicity and immunogenicity. Non-viral systems are safer and more stable but substantially less efficient. Optimizing uptake of these particles is the first step required for achieving efficient non-viral gene delivery.<sup>1-4</sup>

Size, magnetism and transferrin have all been reported as critical in improving non-viral particle uptake. As illustrated in the schematic in figure 1, size can determine the route of uptake by cells<sup>5-13</sup> with larger particles taken up by phagocytosis and smaller particles by endocytosis.<sup>13,14</sup> Different cells can also have different cut-off values for the size of particles that can be taken up.<sup>15</sup> Some reports do not show any link between particle size and transfection ability whilst others show that either small particles<sup>16-18</sup> or large particles are better for *in vitro* transfection.<sup>19-21</sup> Comparison between such results is however complicated by the varying conditions and cell types of each study.

Magnetofection is the delivery of genes by utilization of magnetic forces. It has been shown to result in highly efficient delivery of genes and antisense oligonucleotides.<sup>22,23</sup> and can produce localized gene delivery by the strategic placement of magnets.<sup>24</sup> For *in vitro* applications, magnetofection is particularly useful because of the reported lower incubations time required to achieve transfection, lower vector doses and the possibility of gene delivery to normally non-permissive cells.<sup>22</sup>

Finally, all actively metabolizing cells require iron that is taken up by the cells as a transferrin-iron complex by means of receptor mediated endocytosis. Transferrin has been shown to increase and improve the delivery of drugs, genes and proteins by exploiting this efficient transport mechanism.<sup>4, 25-28</sup>

We have recently reported on a novel non-viral vector based on metallic nanorods that can bind cell targeting proteins such as transferrin and DNA-plasmids in spatially defined regions.<sup>4</sup> The nanorods have several advantages that make them useful in probing the properties that influence transfection efficiency. The ability to increase the length and aspect ratio of the nanorods with specificity allows us to determine the effect of size on transfection efficiency. The magnetic properties of the nickel allow us to explore the potential of magnetofection.<sup>29</sup> The ability to bind transferrin in spatially defined regions without complexation to any other entity ensures that the impact of the cell targeting ability of transferrin on increasing overall transgene expression can be assessed without additional unpredictable variables. In this study, the combination of these properties into

a single delivery device is utilized to provide insights into the relationship between size, transferrin and magnetism in gene delivery.

## **Results and Discussion.**

### **Preparation of nanowires.**

The nanorods were fabricated by electrodeposition into an Al<sub>2</sub>O<sub>3</sub> template (Anodisc, Whatman) with a nominal pore diameter of 100 nm.<sup>30</sup> An evaporated silver film on one side of the template served as the working electrode in a three-electrode configuration. A thin layer of silver was electrodeposited into the template to ensure easy release of the nanorods from the template. Au segments were deposited prior to nickel segments to prevent erosion of the nickel layers during silver removal. The silver layers were dissolved in 70vol % nitric acid and the alumina template was then dissolved in 2 M potassium hydroxide.

Confirmation of deposition of the nickel and gold segments was seen by back-scattering SEM (Fig. 2A). Using chemical moieties that bind selectively to either gold or nickel, we have attached DNA and a cell-targeting protein, transferrin, to the different segments, as reported previously.<sup>4</sup> A small proportion of the primary amine groups of transferrin were converted to sulfhydryl groups. The transferrin was then bound to the gold segments of the nanorods through a thiolate linkage.<sup>31</sup> Electrostatic interactions were used to bind DNA to the nickel segments by suspending the dual component nanorods in a 0.1 M solution of 3-[(2-aminoethyl) dithio] propionic acid (AEDP). The carboxylic acid terminus of AEDP binds to the native oxide on the nickel segments. This results in the surface presentation of primary amine groups spaced by a reducible disulfide linkage. In the reducing environment of the cell, the disulfide linkage between the plasmid and the nanowire is cleavable enhancing release of the plasmid. In this study, plasmids encoding the firefly luciferase (pCMV-luciferase VR1255\_C) with a 6.413 kb driven by the cytomegalovirus (CMV) promoter/enhancer (luciferase plasmid) were utilized. UV-visible spectroscopy calibration measurements (260 nm) of DNA binding to the nickel component of the nanowires provided an average surface coverage of  $4 \times 10^{12}$  molecules/cm<sup>2</sup>. For condensation of the plasmids bound to the nanowires, a CaCl<sub>2</sub> solution was added to the nanowire-plasmid complexes. Ca<sup>2+</sup> has a high affinity to DNA ( $K_d$  of  $1.1 \times 10^{-3} M^{-1}$ ), forming CaPO<sub>4</sub> complexes with the nucleic backbone to provide stabilization and compaction to the DNA structure.

Confirmation of the selective binding of transferrin and plasmid was obtained by fluorescence microscopy on 20 μm long and 170 nm diameter nanorods with Ni and Au segments of equal length. Figure 2b shows a light microscope image of a dual component nanowire with figure 2c highlighting the selective functionalisation with uniform red fluorescence from the rhodamine-tagged transferrin on the gold segments and uniform blue fluorescence from the Hoechst, which specifically binds to the DNA conjugated to the nickel segments.

Nanowire length and width was characterized using back-scattering SEM and J-image software. Nanowires with equivalent nickel and gold sections and lengths ranging

from 100 nm to 6 microns were synthesized with relatively narrow distributions (Table 1). The geometry of the template is structured so that beyond a few hundred nanometers, the 100 nm pores coalesce into pores with larger diameters. For consistency in our studies, we ensured that we deposited silver to fill the pores above the coalescing point prior to gold and nickel deposition.

### **Size, Transferrin and Dose**

For 100 nm nanowires, the immobilization of transferrin resulted in an 11.5 fold increase in transfection efficiency. For 319 nm nanowires, this increase fell to 1.8 fold. The attachment of transferrin to nanowires larger than this did not result in any significant increase in transfection efficiency (Fig. 3). This observation suggests that transferrin cannot catalyze cell internalization of nanorods beyond the reported size dependent restrictions of the receptor mediated endocytic route of uptake.<sup>13, 14, 26</sup>

A broad decrease in transfection was observed with increasing nanowire size. 1  $\mu\text{m}$  nanowires were 15.6 fold less efficient than the 100 nm nanowires (Fig. 4). Because the dose of the nanowires was kept constant (1  $\mu\text{g}$  DNA), we speculated that this may be due to a lower distribution of the nanowires over the cell culture dish e.g. there are 10 times less 1  $\mu\text{m}$  nanowires at a 1  $\mu\text{g}$  DNA dose than there are for a 1  $\mu\text{g}$  DNA dose of 100 nm nanowires.

To test this hypothesis, 293HEK cells were incubated with a constant number of nanowires regardless of size and aspect ratio. As a result, there was an increasing DNA dose with increasing length of nanowires. 1  $\mu\text{m}$  nanowires (20  $\mu\text{g}$  DNA) produced equivalent transfection efficiencies to a 2  $\mu\text{g}$  DNA dose of 100 nm nanowires (Fig. 4A). However, the 1  $\mu\text{m}$  nanowires also produced a notable decrease in protein content in comparison to the 100 nm nanowires (Fig. 4B). Similarly, a 10-fold increase in DNA dose with the 100 nm nanowires from 2  $\mu\text{g}$  to 20  $\mu\text{g}$  resulted in a 9.3 fold increase in transfection (Fig. 4A) but also resulted in a toxicity associated decrease in cell viability from 99.1% to 57.1% as determined by protein content (Fig. 4B).

### **Size and route of uptake**

The fact that transferrin is an efficient cell targeting protein for small nanowires but not larger nanowires indicates that the size not only influences transfection efficiency but also the mechanism of uptake. Consistent with our previous results, we found that single 100-200 nm nanowires could be found in endosomal/lysosomal type vesicles by TEM analysis.<sup>4</sup> This route of uptake is generally achieved by small particles bound to pits on the cell membrane that invaginate to pinch off forming vesicles.<sup>13, 14</sup> However, aggregated nanowires were also observed in multivesicular entities or larger phagosome type vesicles. Given that the size limit of particles for transferrin-mediated endocytosis has been reported to be in the region of 150-200 nm<sup>1</sup> and we have found that endosome vesicles have diameters approximately 200–250 nm, it seems most likely that uptake of these aggregated nanowires is due to a mechanism other than endocytosis possibly phagocytosis.<sup>32</sup> The larger nanowires were also found in larger more phagocytic type vesicles. Previous reports have shown that a number of cell types including epithelial,

fibroblast and endothelial cells can take up large particles *in vitro* through this mechanism.<sup>1,33-35</sup>

## **Magnetism and Transferrin**

Magnetofection is a useful tool in gene delivery because it can ensure that the bulk of the vectors in solution reach the cell surface resulting in a significantly improved dose-response profile.<sup>22</sup> When we applied a NdFeB magnet to the bottom of a culture dish containing 100nm nanorods during the 4hr transfection period, we observed a 3-fold increase in transfection efficiency (Fig. 5). TEM sections did not reveal any difference in the mechanism of uptake indicating that this increase in expression was due to accelerated sedimentation of the vectors to the surface of the cell consistent with the observations by others.<sup>36,37</sup> Of further interest, when transferrin was added to the 100 nm nanorods without a magnetic field, we observed a 4-fold increase in transfection. The combination of transferrin immobilization and a magnetic field resulted in a 5.25 fold increase in transfection. Transferrin in addition to promoting cellular internalization may also be increasing transfection by simply increasing the binding of the nanowires to the surface of the cell facilitating uptake by other mechanisms. This concept is consistent with the observations of Wagner and colleagues who showed that transferrin could increase transfection efficiencies despite using particles that were circa 500nm, which is a size that is greater than the cut-off point for clathrin-mediated endocytosis of particles.<sup>19</sup> The lack of increase in transfection when transferrin is bound to nanowires larger than 600 nm (Fig. 3) may represent a greater difficulty to binding of receptors on the surface of the cell which are generally found inside pits that are no greater than a few hundred nanometers in diameter.<sup>13,14</sup> A possible explanation for why transferrin does not improve transfection significantly in the presence of a magnetic field is that the magnetic field may be orientating the nanorods so that the nickel portion faced towards the cell surface and thus the transferrin receptors would be facing away from the cell surface negating their benefits. We are currently in the process of preparing a system with greater control over the magnetic field gradients that should improve transfection efficiencies even further.

## **Size and Particle Bombardment**

Gene gun delivery of nanoparticles is a particularly efficient method because it involves bombardment directly into the cytoplasm. Thus, the traditional routes of particle uptake such as phagocytosis and endocytosis are completely bypassed. The overall transfection efficiencies of this delivery method were an order of magnitude higher than incubating nanowires. In direct contrast to incubation with nanowires, we found in gene gun delivery that increasing the nanowire size from 100 nm to 1 micron at a constant pressure of 250 psi resulted in higher transfection efficiency (Fig. 6A). However, increasing the length of nanowires above 1  $\mu\text{m}$  began to produce lower transfection efficiencies with associated increases in toxicity (Fig. 6B). Wires larger than 1  $\mu\text{m}$  are presumably causing greater cell damage that offsets the benefits of their higher mass.

To identify if increasing pressure improves the transfection efficiency of the 100 nm nanowires, we increased the pressure from 250 psi to 600 psi. Increasing pressure

resulted in decreasing cell viability from 82% (250 psi) to 48% (400 psi) to 14% (600 psi) (Fig. 6C). These protein content measurements corresponded to the observation of few live cells in the blast zone at higher pressures. Finally addition of transferrin to the nanorods did not result in significant increases (by ANOVA analysis) in transfection for any nanorod length. This is consistent with the concept of the gene gun bypassing endocytosis thus negating the requirement of cell receptors that promote this route of uptake.

## Conclusions.

Size of particles can determine route of uptake with larger particles phagocytosed and smaller particles endocytosed or taken up by macropinocytosis. The size of the particle also impacts on transfection efficiency. Smaller nanowires are more efficient using standard methods of *in vitro* incubation, whilst larger nanowires are more efficient by particle bombardment. There is a cut-off size that transferrin can be used as a cell targeting protein and it has no benefits in gene gun delivery methods where the endocytic route is bypassed. Magnetofection does not alter the route of uptake but simply accelerates the particle to the cell surface increasing the physical concentration of nanorods and helping to bind them on the cell surface.

## Methods and Materials

### Preparation of 200nm dual component Au/Ni nanowires

Nanowires were fabricated by electrodeposition into an Al<sub>2</sub>O<sub>3</sub> template (Anodisc, Whatman) with a nominal pore diameter of 100 nm. An evaporated silver film on one side of the template served as the working electrode in a three-electrode configuration. A thin layer of silver was first electrodeposited from 50 mM KAg(CN)<sub>2</sub> and 0.25 M Na<sub>2</sub>CO<sub>3</sub> buffered to pH 13 at a potential of -1.0 V (Ag/AgCl) in order to ensure easy release of the nanowires from the template. The Au segments were deposited from a commercial gold plating solution (Technic) at a potential of -1.0 V (Ag/AgCl) and the Ni segments were deposited from a solution of 20 g L<sup>-1</sup> NiCl<sub>2</sub> · 6H<sub>2</sub>O, 515 g L<sup>-1</sup> Ni(H<sub>2</sub>NSO<sub>3</sub>)<sub>2</sub> · 4 H<sub>2</sub>O, 20 g L<sup>-1</sup> H<sub>3</sub>BO<sub>3</sub> buffered to pH 3.4 at a potential of -1.0 V (Ag/AgCl). The silver layers were dissolved in 70 vol. % nitric acid and the alumina template was then dissolved in 2 M KOH. The nanowires were washed repeatedly using 2 M KOH, de-ionized water, and ethanol.

### DNA binding.

A 150 µl of 0.1 M AEDP (Pierce) solution was added to 200 µl aliquots of nanorods (~ 1 x 10<sup>6</sup>) suspended in distilled water. Following incubation for 24 h and washing, 2 µg of plasmid was added to each aliquot of nanorods, (pH 5.7) and incubated at 4 °C for 24 h. After washing, 2 µl of a 2M CaCl<sub>2</sub> solution was added to each aliquot and then incubated for 24 h at 4 °C. For fluorescent staining of plasmids, nanorods were incubated with 100 µl of a 0.01 mg ml<sup>-1</sup> Hoechst 33258 (Bisbenzimidazole, Molecular Probes). Absorbance spectroscopy on the DNA bound to nanowires was measured at 260 nm.

### **Transferrin binding.**

5 mg of rhodamine-conjugated transferrin (Molecular probes) in PBS with 5 mM EDTA was reacted with 120  $\mu\text{l}$  of 5 mg  $\text{ml}^{-1}$  iminothiolane (Pierce) for 30 minutes at room temperature. The protein was purified by dialysis at 4 °C. Twenty  $\mu\text{l}$  of 5 mg  $\text{ml}^{-1}$  rhodamine-transferrin-SH was added to each aliquot of nanorods and incubated for 24 h at 4 °C.

### **Transfection experiments**

HEK293 cells (ATCC) were cultured in T75 flasks in DMEM with 10% FCS and ABAM. All cell culture and Lipofectamine reagents were purchased from Gibco BRL, Rockville, MD. The serum-containing media was replaced every 3 days and split 1:3 at pre-confluence. The luciferase encoded plasmids were a gift from Dr Carl Wheeler, Vical Incorporated. HEK293 cells were seeded onto 24-well plates ( $3 \times 10^5$  cells/well). Each well (24-well) was transfected in 0.5 ml reduced-serum Opti-MEM media.

Lipofectamine: DNA complexes at a ratio of 4:1 using 8  $\mu\text{g}$  Lipofectamine in 40  $\mu\text{l}$  Opti-MEM and 2  $\mu\text{g}$  DNA in 40  $\mu\text{l}$  Opti-MEM was added to control wells. Forty  $\mu\text{l}$  of the nanorods/DNA suspension was added per well. After 4 h, the transfection media was removed and the cells washed. After 2 days, the cells were washed with PBS. 150  $\mu\text{l}$  of lysis buffer (5x diluted to 1x using distilled water) was then added to each well for 15 minutes to permeabilise the cells. The cells were then scraped vigorously to remove them from the surface of the well. This cell debris was then transferred to plastic eppendorf and centrifuged for 12,000 rpm for 10 minutes. Luciferase activity was then measured using the luminometer for 10 secs using 20  $\mu\text{l}$  of each sample supernatant with 50  $\mu\text{l}$  of luciferase assay reagent (LAR). This was mixed quickly and tested for chemiluminescence intensity using a luminometer (EG&G Berthold MiniLumat). Each RLU value was noted before moving onto the next sample. Following this, a protein content assay was carried out on the supernatant using standard BCA protocols (Biorad). Modifications include the use of cell lysis buffer as the diluents. Following preparation of the standards, and the samples, 96 well plates (each well containing 25  $\mu\text{l}$  of sample) was placed on the colorimetric plate reader and read using the 570 filter. Using the BioRad protein assay kit, a calibration curve was formed that determined the total cell protein content and the RLU values from luciferase activity were then converted to RLU/mg of protein/min. For TEM studies on internalization, cells were fixed with 2% glutaraldehyde/ 2% paraformaldehyde in PBS at selected time-points. After washing with PBS, cells were dehydrated with graded ethanol and coated with 2% osmium tetroxide (Aldrich). TEM samples were sectioned in epoxy resin by microtome and developed using 2% uranyl acetate and 0.04% lead citrate. TEM analysis was performed using a Philips CM-300 FEG. For magnetofection studies, neodymium-iron-boron (Nd-Fe-B) permanent magnet plates were placed under cell culture plates during transfection. The magnetic gradient fields were checked to ensure that vectors accelerated to the surface.

### **Delivery of nanowires by gene gun**

Nanowire-DNA complexes and Nanowire-Transferrin-DNA complexes at varying concentrations to keep DNA dose constant were added to a 1.5 ml microfuge tube and

centrifuged for 15 seconds to pellet the nanowires. The supernatant was discarded. The pellet was washed three times with 1ml of fresh ethanol each time; spun for 5 seconds between each wash with the supernatant discarded. After the final wash, the pellet was resuspended in 200  $\mu$ l of ethanol and transferred to a 15 ml disposable polypropylene centrifuge tube with a screw cap. 3.5 ml of ethanol was added to this. 17.5  $\mu$ l of a 20 mg/ml PVP in ethanol solution was added to this and the mixture vortexed. Parafilm was wrapped round the cap to seal the tubes. To load the cartridges with the nanowire solution, a tubing prep station was connected to a nitrogen tank. A 10 cc syringe was fitted with a 16-18" piece of silicone adaptor tubing and inserted into the syringe sleeve and clamped onto the base of the tubing prep station to remove the liquid from the nanowire-coat tubing. Prior to preparing cartridges, the nanowire-coat tubing was completely dried with nitrogen for 15 minutes. For this, the tubing was inserted into the tubing support cylinder. The nitrogen flow rate was set at 0.35 LPM. The nanowire-coat tubing was removed from the tubing prep station and the nitrogen supply closed. A 30" length of tubing was cut for each 3.5ml sample of nanowire/DNA suspension with one end attached to the 10 cc syringe. The nanowire suspension was vortexed briefly and the tube inverted several times to resuspend the nanowires before quickly drawing nanowires suspension into the nanowire-coat tubing approximately 23" from the end leaving 3" at each end. The nanowire-coat tubing was brought to a horizontal position and the loaded tube slid with syringe attached into the tubing support cylinder in the Tubing prep station. The nanowires were allowed to settle for 3-5 minutes. The liquid was then removed at 0.5-1"/sec for 25-45 seconds until all the liquid had been removed from the tube. The syringe was detached and the nanowires-coat was rotated 180 degrees while in the groove allowing the nanowires to begin coating the inside of the tubing for 3-4 seconds. The nanowire-coat tube was then rotated. The nanowires smeared the tube for 20-30 seconds after which the nitrogen flow was switched on at 0.4 LPM whilst the tubing was still rotating. The tube was dried for a further 5 minutes. For tubing where the nanowires were evenly distributed, the tubes were cut into 0.5" pieces using a tubing cutter.

The Helios gene gun was loaded with the cartridges and connected to a helium source with the pressure set at 250 psi. The gene gun was discharged two or three times prior to use. Immediately prior to DNA delivery, media was aspirated from the dish. The dish was held as close as possible perpendicular to a sterilized spacer and the gene gun discharged. 2ml of media was added to the dish and returned to the incubator. This procedure was repeated for all the samples.

## References

- (1) Zauner, W.; Farrow, N. A.; Haines, A. M. R. *Journal of Controlled Release* **2001**, *71*, 39-51.
- (2) Luo, D.; Saltzman, W. M. *Nature Biotechnology* **2000**, *18*, 33-37.
- (3) Roy, K.; Mao, H. Q.; Huang, S. K.; Leong, K. W. *Nature Medicine* **1999**, *5*, 387-391.
- (4) Salem, A. K.; Searson, P. C.; Leong, K. W. *Nature Materials* **2003**, *2*, 668-671.
- (5) Steinkamp, J. A.; Wilson, J. S.; Saunders, G. C.; Stewart, C. C. *Science* **1982**, *215*, 64-66.
- (6) Oda, T.; Maeda, H. *Journal of Immunological Methods* **1986**, *88*, 175-183.
- (7) Jani, P.; Halbert, G. W.; Langridge, J.; Florence, A. T. *Journal of Pharmacy and Pharmacology* **1990**, *42*, 821-826.
- (8) Griese, M.; Reinhardt, D. *Journal of Drug Targeting* **1998**, *5*, 471-+.
- (9) Ogawara, K.; Yoshida, M.; Higaki, K.; Kimura, T.; Shiraishi, K.; Nishikawa, M.; Takakura, Y.; Hashida, M. *Journal of Controlled Release* **1999**, *59*, 15-22.
- (10) Pratten, M. K.; Lloyd, J. B. *Biochimica Et Biophysica Acta* **1986**, *881*, 307-313.
- (11) Fujita, H.; Ueda, A.; Nishida, T.; Otori, T. *Cell and Tissue Research* **1987**, *250*, 251-255.
- (12) Schroeder, F.; Kinden, D. A. *Journal of Biochemical and Biophysical Methods* **1983**, *8*, 15-27.
- (13) Conner, S. D.; Schmid, S. L. *Nature* **2003**, *422*, 37-44.
- (14) Marsh, M.; McMahon, H. T. *Science* **1999**, *285*, 215-220.
- (15) Zauner, W.; Ogris, M.; Wagner, E. *Advanced Drug Delivery Reviews* **1998**, *30*, 97-113.
- (16) Desai, M. P.; Labhasetwar, V.; Walter, E.; Levy, R. J.; Amidon, G. L. *Pharmaceutical Research* **1997**, *14*, 1568-1573.
- (17) Kreiss, P.; Cameron, B.; Rangara, R.; Mailhe, P.; Aguerre-Charriol, O.; Airiau, M.; Scherman, D.; Crouzet, J.; Pitard, B. *Nucleic Acids Research* **1999**, *27*, 3792-3798.
- (18) Prabha, S.; Zhou, W. Z.; Panyam, J.; Labhasetwar, V. *International Journal of Pharmaceutics* **2002**, *244*, 105-115.
- (19) Ogris, M.; Steinlein, P.; Kursa, M.; Mechtler, K.; Kircheis, R.; Wagner, E. *Gene Therapy* **1998**, *5*, 1425-1433.
- (20) Niidome, T.; Ohmori, N.; Ichinose, A.; Wada, A.; Mihara, H.; Hirayama, T.; Aoyagi, H. *Journal of Biological Chemistry* **1997**, *272*, 15307-15312.
- (21) Emi, N.; Kidoaki, S.; Yoshikawa, K.; Saito, H. *Biochemical and Biophysical Research Communications* **1997**, *231*, 421-424.
- (22) Scherer, F.; Anton, M.; Schillinger, U.; Henkel, J.; Bergemann, C.; Kruger, A.; Gansbacher, B.; Plank, C. *Gene Therapy* **2002**, *9*, 102-109.
- (23) Krotz, F.; de Wit, C.; Sohn, H. Y.; Zahler, S.; Gloe, T.; Pohl, U.; Plank, C. *Molecular Therapy* **2003**, *7*, 700-710.
- (24) Pandori, M. W.; Hobson, D. A.; Sano, T. *Virology* **2002**, *299*, 204-212.

- (25) Wagner, E.; Curiel, D.; Cotten, M. *Advanced Drug Delivery Reviews* **1994**, *14*, 113-135.
- (26) Wagner, E.; Zenke, M.; Cotten, M.; Beug, H.; Birnstiel, M. L. *Proceedings of the National Academy of Sciences of the United States of America* **1990**, *87*, 3410-3414.
- (27) Truong-Le, V. L.; August, J. T.; Leong, K. W. *Human Gene Therapy* **1998**, *9*, 1709-1717.
- (28) Mao, H. Q.; Roy, K.; Troung-Le, V. L.; Janes, K. A.; Lin, K. Y.; Wang, Y.; August, J. T.; Leong, K. W. *Journal of Controlled Release* **2001**, *70*, 399-421.
- (29) Whitney, T. M.; Jiang, J. S.; Searson, P. C.; Chien, C. L. *Science* **1993**, *261*, 1316-1319.
- (30) Sun, L.; Searson, P. C.; Chien, C. L. *Applied Physics Letters* **2001**, *79*, 4429-4431.
- (31) Laibinis, P. E.; Hickman, J. J.; Wrighton, M. S.; Whitesides, G. M. *Science* **1989**, *245*, 845-847.
- (32) Rabinovitch, M. *Trends in Cell Biology* **1995**, *5*, 85-87.
- (33) Goldman, R. *Experimental Cell Research* **1977**, *104*, 325-334.
- (34) Ryan, U. S.; Schultz, D. R.; Goodwin, J. D.; Vann, J. M.; Selvaraj, M. P.; Hart, M. A. *Infection and Immunity* **1989**, *57*, 1356-1362.
- (35) Nepomuceno, R. R.; Tenner, A. J. *Journal of Immunology* **1998**, *160*, 1929-1935.
- (36) Plank, C.; Schillinger, U.; Scherer, F.; Bergemann, C.; Remy, J. S.; Krotz, F.; Anton, M.; Lausier, J.; Rosenecker, J. *Biological Chemistry* **2003**, *384*, 737-747.
- (37) Luo, D.; Saltzman, W. M. *Nature Biotechnology* **2000**, *18*, 893-895.

Figure 1. Size-dependent routes of entry into cell

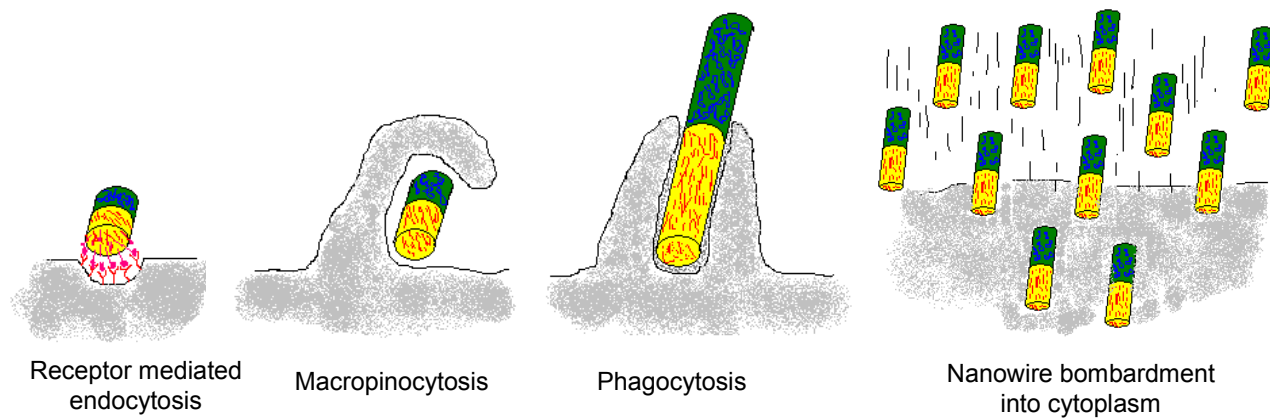


**Figure 2A.** Back-scattered SEM image of two component Au/Ni nanorods. Confirmation of selective functionalisation of nanorods is observed by light and fluorescent microscopy. **B,** Light microscope image of dual functionalized 20  $\mu\text{m}$  long Au/Ni nanorod. **C,** Fluorescence overlay image of the rhodamine-tagged (633 nm) transferrin on the Au segment and the Hoechst stained (350/450 nm) plasmids on the Ni segment.

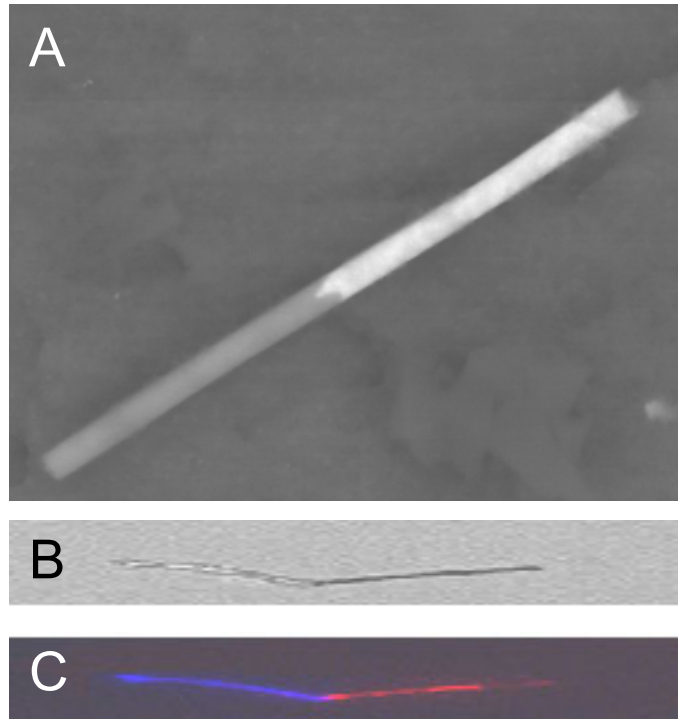


**Figure 3.** Log plot of nanorod size effects on transfection efficiency with (●) and without transferrin immobilization (○)

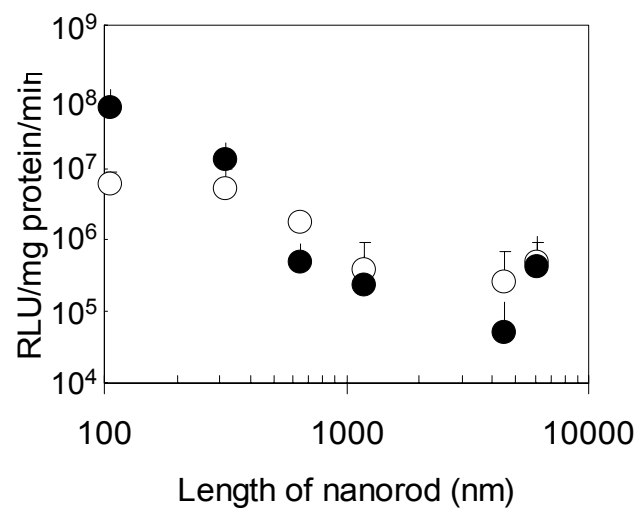


**Figure 4.** Results of transfection experiments comparing dose and size of nanorods

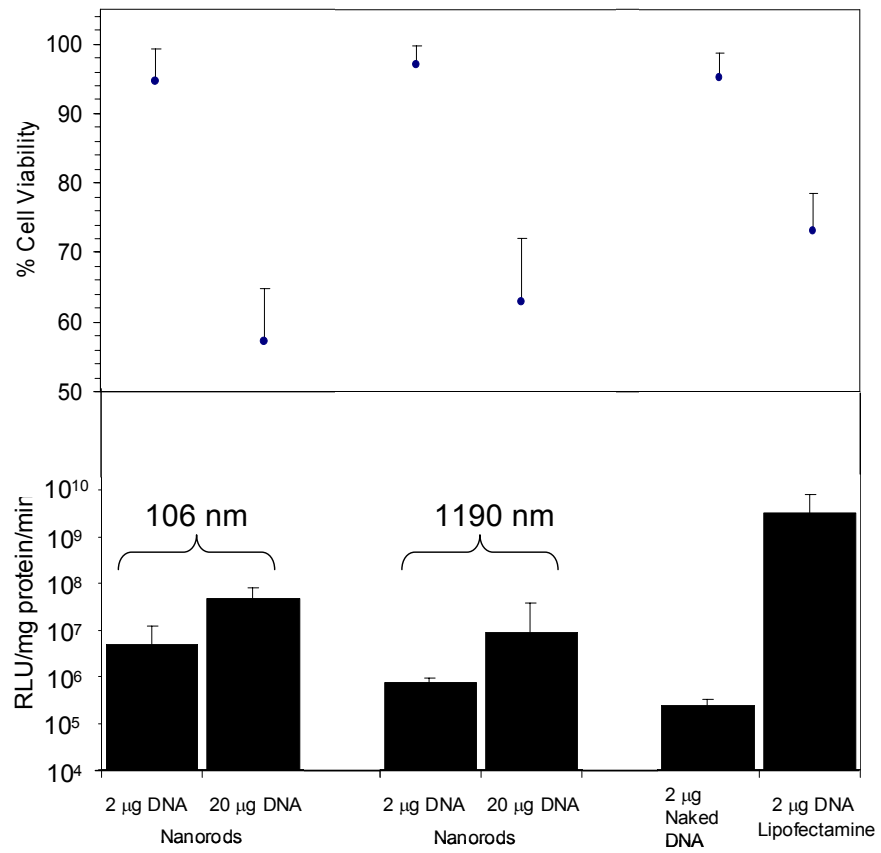


**Figure 5.** Results of transfection experiments comparing the effects of a magnetic field on nanorods with and without transferrin

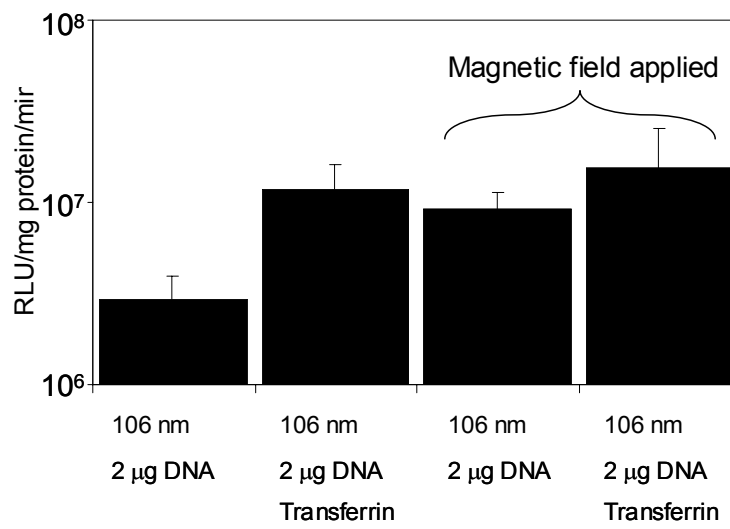


**Figure 6A.** Log plot of nanorod size effects on transfection efficiency with (●) and without transferrin immobilization (○) by gene gun delivery. **Figure 6B.** Viability of cells when exposed to gene gun bombardment of 106 nm nanorods at varying pressures determined by protein content and normalized to control cells without treatment. At 250 psi, an additional group was tested with a shield provide extra protection at the center of the blast zone. **Figure 6C.** Viability of cells with gene gun delivery at 250 psi of varying nanorod sizes determined by protein content and normalized to control cells without treatment.

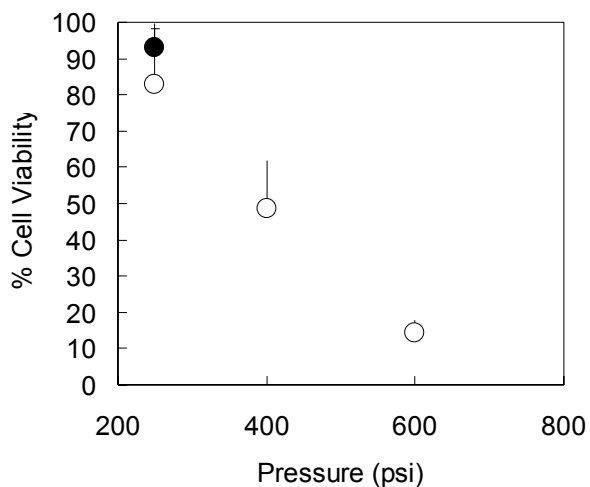
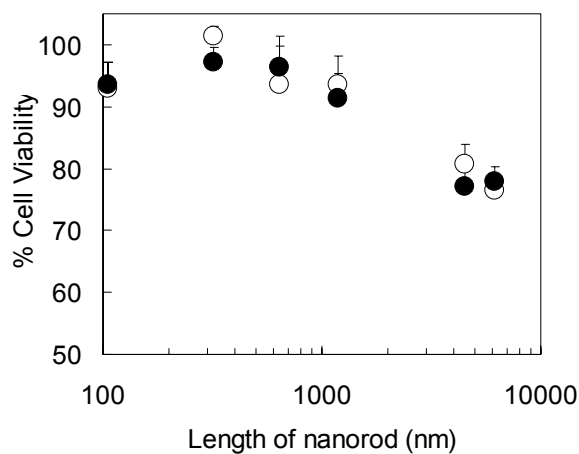
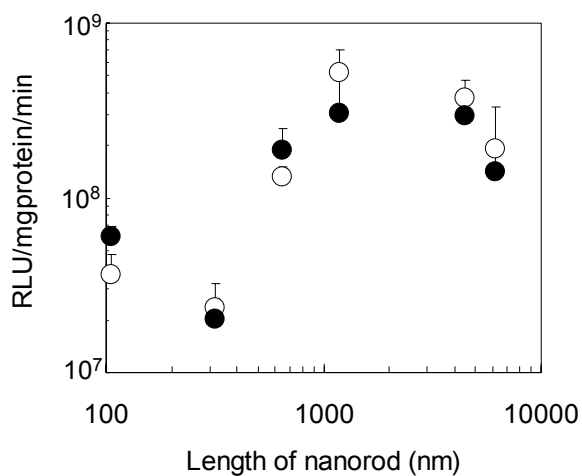


**Table 1.** Summary of nanowire size characterization.

Group	Mean Length (nm) $\pm$ SD (min-max)	Diameter Mean (nm) $\pm$ SD (min-max)	Length Nickel (nm) $\pm$ SD (% Ni)	Length Gold (nm) $\pm$ SD (% Au)
1	106 $\pm$ 13.7 (77.5 – 128)	167 $\pm$ 24.4 (119 – 195)	37.6 $\pm$ 8.43 (47.8%)	61.2 $\pm$ 7.83 (52.3%)
2	319 $\pm$ 39 (286 - 417)	133 $\pm$ 31.7 (91.5 – 190)	148 $\pm$ 24.3 (45.5%)	176 $\pm$ 18 (54.5%)
3	643 $\pm$ 32.2 (575 - 687)	161 $\pm$ 24.9 (121 – 206)	255 $\pm$ 30.2 (42.8%)	343 $\pm$ 52 (57.2%)
4	1190 $\pm$ 175 (942 - 138)	223 $\pm$ 41.9 (162 – 306)	476 $\pm$ 117 (39.7%)	715 $\pm$ 106 (60.3%)
5	4480 $\pm$ 387 (4000 - 5090)	143.66 $\pm$ 17.03 (106 – 165)	1880 $\pm$ 253 (41.9%)	2600 $\pm$ 199 (58.1%)
6	6130 $\pm$ 923 (5000 - 7820)	231 $\pm$ 43 (175 - 313)	2580 $\pm$ 518 (40.4%)	3785 $\pm$ 561 (59.6%)